Influence of oxygen and hydrogen adsorption on the magnetic structure of an ultrathin iron film on an Ir(001) surface

František Máca,[1,*] Josef Kudrnovský,[1] Václav Drchal,[1] and Josef Redinger[2]
[1]*Institute of Physics ASCR, Na Slovance 2, CZ-182 21 Praha 8, Czech Republic*
[2]*Department of Applied Physics, Vienna University of Technology, Gusshausstrasse 25/134, 1040 Vienna, Austria*
(Received 7 June 2013; published 15 July 2013)

We present a detailed *ab initio* study of the electronic structure and magnetic order of an Fe monolayer on the Ir(001) surface covered by adsorbed oxygen and hydrogen. The results are compared to the clean Fe/Ir(001) system, where recent intensive studies indicated a strong tendency towards an antiferromagnetic order and complex magnetic structures. The adsorption of an oxygen overlayer significantly increases interlayer distance between the Fe layer and the Ir substrate, while the effect of hydrogen is much weaker. We show that the adsorption of oxygen (and also of hydrogen) leads to a $p(2 \times 1)$ antiferromagnetic order of the Fe moments, which is also supported by an investigation based on a disordered local moment state. Simulated scanning tunneling images using the simple Tersoff-Hamann model hint that the proposed $p(2 \times 1)$ antiferromagnetic order could be detected even by nonmagnetic tips.

DOI: 10.1103/PhysRevB.88.045423 PACS number(s): 75.30.−m, 81.20.−n

I. INTRODUCTION

Magnetic overlayers, i.e., thin films of magnetic materials on a nonmagnetic substrate, prepared by molecular beam epitaxy, represent a new type of material with potential technological applications. Among a number of such systems, recently the fcc-Fe/Ir(001) overlayer system has attracted both experimental and theoretical attention. Thin overlayers were grown successfully with negligible Fe-Ir intermixing. A metastable unreconstructed monolayer (ML) of Fe on the Ir(001) surface could be prepared[1,2] and studied theoretically by *ab initio* methods.[3,4] Both theoretical investigations predicted a complex magnetic ground state. It should also be noted that complex chiral magnetic structures were also observed for a related bcc-Fe/W(001) system.[5]

Concerning adsorption, oxygen and hydrogen are the two most likely adsorbates to exist on Fe/Ir(001) surfaces. The investigation of their influence on the structural, electronic, and magnetic ground state is thus an interesting and relevant problem. We like to mention here a related recent experimental and theoretical study of an oxygen covered bcc-Fe(001) surface,[6] where experiment confirms the formation of a well-defined monolayer where the oxygens occupy the fourfold coordinated hollow positions and stabilize the ferromagnetic (FM) state. The situation is richer and even more interesting in the present fcc-Fe/Ir(001) case because oxygen adsorption can influence the Fe-Ir distance and thus also the magnetic ground state which sensitively depends on.[3] In contrast, hydrogen, which is likely to be present due to the preparation of the Fe/Ir(001) samples,[1] adsorbs and hybridizes differently from oxygen.

The ground state structure including possible layer relaxations is determined by conventional *ab initio* tools (the supercell VASP method,[7] for more details see the next section). The magnetic ground state is predicted on the basis of the Heisenberg model with exchange interaction parameters determined from first principles. Two approaches are used: (i) in the first one, two effective pair interactions are obtained utilizing the total energies of the ferromagnetic (FM) and two antiferromagnetic (AFM) configurations [$c(2 \times 2)$ and $p(2 \times 1)$] for the respective relaxed structural models calculated by VASP; and (ii) the disordered-local moment (DLM) state is used as a reference state for the extraction of exchange interactions as done in a previous paper[3] for the clean Fe/Ir(001) system. The input electronic structure for the DLM state employs a realistic semi-infinite geometry and the tight-binding linear muffin-tin orbital (TB-LMTO) method in the Green function formulation. The DLM state is simulated in the alloy analogy approximation (for more details see Ref. 3 and references therein). We used the geometry as obtained by the atomic force minimization of VASP and chose the radii of the atomic spheres in order to minimize their overlap. The above two approaches for the estimation of the exchange interactions are complementary to each other, the former one is more accurate, but since it employs only three magnetic configurations, its predictions are limited to the simplest magnetic structures and more complex configurations may thus be missed. We demonstrate this for a monolayer of Fe on the Ir(001) surface. The latter approach, based on the DLM method, does not assume any specific magnetic structure and takes into account a large number of exchange integrals (which in a two-dimensional case decay more slowly with distance than in the bulk case[8]). The DLM approach using the TB-LMTO method is, however, less accurate, in particular for the case of small interlayer adsorbate-iron distances. Finally, STM images simulating the constant current measuring mode of STM were calculated using the Tersoff-Hamann approximation,[9] where tip-sample interactions are neglected and thus the tip is supposed to follow the contours of a constant density of states contained in an energy interval given by E_F and the applied bias voltage V_{Bias}.

II. COMPUTATIONAL DETAILS

First-principles density functional theory calculations were performed using the Vienna *ab initio* simulation package VASP[7] using the projector augmented wave scheme[10] and

local density approximation (LDA) as given by Perdew-Zunger (Ceperly-Alder).[11] Repeated asymmetric slabs with seven layers of Ir and a single Fe monolayer on one side and also symmetric slabs with 11 substrate layers and adsorbate layers on both sides were used, separated by at least 19 Å vacuum. Three top layer distances have been relaxed, the remaining interlayer distances were fixed to the bulk experimental value for the Ir crystal (1.92 Å). The calculated relaxations turned out to be essentially the same for both setups. We have tested the FM, $c(2 \times 2)$ AFM, and $p(2 \times 1)$ AFM arrangements, all performed with four Fe/Ir atoms in the two-dimensional supercell to guarantee a reliable comparison of total energies. Technically we have used a Brillouin zone sampling with 100–200 special k points in the irreducible two-dimensional wedge. The allowed error in total energy was 0.05 meV. The total force on single atoms was in every case smaller than 2.5 meV/Å.

The input electronic structure for the DLM state was determined for a realistic semi-infinite geometry in the framework of the TB-LMTO method and the Green function formulation. The same LDA functional as in VASP calculations was used[11] together with layer relaxations as obtained by VASP and atomic sphere radii chosen to minimize their overlap. The vacuum above the overlayer was simulated by empty spheres (ES). Electronic relaxations were allowed in three empty sphere layers adjoining the oxygen overlayer, in the oxygen and iron layers, and in five adjoining Ir substrate layers. This finite system was sandwiched self-consistently between the frozen semi-infinite fcc-Ir(001) bulk and the ES vacuum space including the dipole surface barrier. For more details see Ref. 3 and references therein.

The effective exchange integrals J_1 and J_2 were estimated in the *total energy model* from total energies calculated for three different magnetic configurations as follows:

$$\begin{aligned} J_1 &= \tfrac{1}{8}\left[E^{\rm tot}_{c(2\times2)}({\rm AFM}) - E^{\rm tot}_{c(2\times2)}({\rm FM})\right], \\ J_2 &= \tfrac{1}{8}\left[E^{\rm tot}_{p(2\times1)}({\rm AFM}) - E^{\rm tot}_{p(2\times1)}({\rm FM}) - 4J_1\right], \end{aligned} \tag{1}$$

where corresponding energies were obtained for the calculated equilibrium atomic structure and indicated magnetic phase. We note that on the square lattice the most probable magnetic configurations are employed.

In the *DLM model* the exchange integrals $J^{\rm Fe,Fe}_{i,j}$ between sites i,j in the magnetic overlayer are expressed as follows (the generalized Liechtenstein formula) (see, e.g., Ref. 12):

$$J^{\rm Fe,Fe}_{i,j} = \frac{1}{4\pi}\,{\rm Im}\int_C {\rm tr}_L\left[\Delta^{\rm Fe}_i(z)\, g^{\uparrow}_{i,j}(z)\, \Delta^{\rm Fe}_j(z)\, g^{\downarrow}_{j,i}(z)\right] dz. \tag{2}$$

Here the trace extends over s, p, and d basis sets, the quantities $\Delta^{\rm Fe}_i$ are proportional to the calculated exchange splittings, and the Green function $g^{\sigma}_{i,j}$ describes the propagation of electrons of a given spin ($\sigma = \uparrow, \downarrow$) between sites i,j, both in the magnetic layer and via the Ir substrate.

Once the exchange interactions are known, we construct the corresponding two-dimensional (2D) Heisenberg model in which only interactions between iron moments are included explicitly and the interactions with iridium atoms and with the adsorbate are included indirectly via self-consistent electronic structure calculations. In the next step we determine its lattice Fourier transform J($\mathbf{q}$) using calculated exchange interactions up to 90 nearest neighbors. The wave vector $\mathbf{q}_0$ in the 2D Brillouin zone at which it acquires its maximum determines the theoretically predicted magnetic ground state.[3]

The STM simulations using the Tersoff-Hamman approach[9] were done with VASP using the optimum geometry as determined before. A fine k-point mesh of $20 \times 40 \times 1$ on an Γ-centered grid was used to sample the 2D Brillouin zone and the energy cutoff was increased up to 600 eV to ensure a smooth numerical representation even for the small values of the charge density in the vacuum region. Energy slices according to the applied bias voltage, i.e., states between $E_{\rm F}$ and $V_{\rm Bias}$, were considered. A typical charge density contour of 10^{-6} e Å^{-3} puts a presumed tip at a distance of ∼3–4 Å above the terminal O atoms, a value not too far from experimental distances. In order to simulate experimental conditions using nonmagnetic tips, the images are obtained from spin averaged densities.

III. RESULTS AND DISCUSSION

A. Atomic structure

In the following we present the results for possible ground state adsorbate structures. All calculations here were done using the VASP-LDA method and the experimental bulk lattice constant for fcc Ir to facilitate a direct comparison with our previous study.[3] This choice of exchange-correlation potential may lead to some underestimation of the absolute values of interlayer distances for the adsorbates since the experimental value (3.84 Å) is slightly larger than the theoretical one (3.82 Å). On the other hand, the trends like, e.g., an increase/decrease of interlayer distances due to the adsorbate are predicted correctly. In Table I we summarize layer relaxations for various investigated systems. Only the results for configurations minimizing the total energy are presented.

It is well known that oxygen atoms favor the occupation of the fourfold hollow Fe sites (see, e.g., Ref. 6 and references therein). This site preference is also reproduced by our VASP calculations, which put the O atoms directly above the substrate Ir atoms. Figure 1 shows that for 1 ML oxygen coverage a $p(2 \times 1)$ AFM magnetic order of Fe magnetic moments is preferred ($E^{c(2\times2)}_{\rm AFM} > E_{\rm FM} > E^{p(2\times1)}_{\rm AFM}$, $\Delta E_{\rm tot} =$

TABLE I. Calculated interlayer distances d_{ij} between top three sample layers for ground state magnetic configurations of Fe/Ir(001), O on Fe/Ir(001), and H on Fe/Ir(001) in the AFM states. b_i represents the buckling of the atoms in layer i. Oxygen is adsorbed in a hollow site and hydrogen on a favorable bridge position. LEED experimental values are taken from Refs. 1 and 2.

	d_{12} (Å)	d_{23} (Å)	d_{34} (Å)	d_{45} (Å)	b_3 (Å)
$c(2 \times 2)$Fe	1.55	1.97	1.88	1.92	0.00
1 ML O on $p(2 \times 1)$Fe	0.59	1.98	1.86	1.90	0.00
0.5 ML O on $p(1 \times 2)$Fe	0.72	1.74	1.91	1.92	0.17
0.5 ML H on $p(2 \times 1)$Fe	1.12	1.59	1.92	1.92	0.17
Fe (expt.)	1.69	1.96	1.91	1.92	–
H on Fe (expt.)	–	1.72	1.94	1.91	–

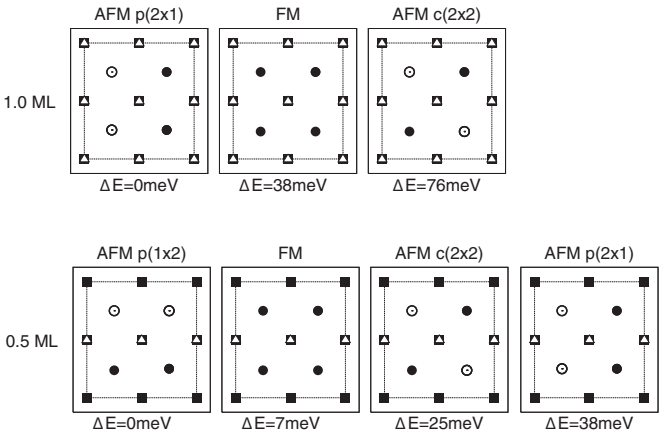

FIG. 1. Schematic structure of 1 ML (top row) and 0.5 ML oxygen (bottom row) on a magnetic Fe/Ir(001) surface. Squares mark the topmost Ir substrate atoms, circles mark the Fe atoms (full/empty denote up/down spin), and white triangles mark the oxygen atoms. The energy difference per Fe atom with respect to the lowest energy solution is indicated beneath each configuration.

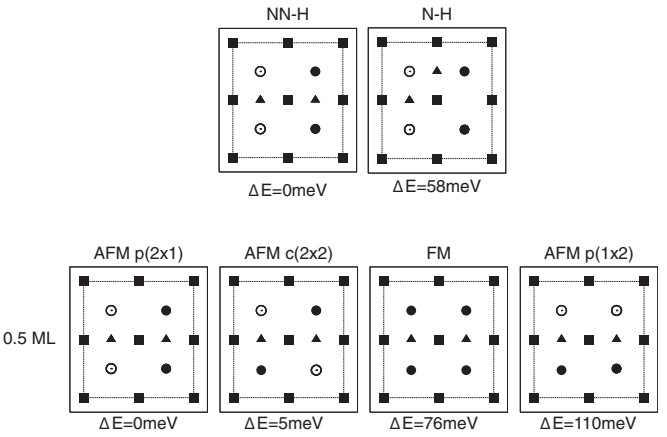

FIG. 2. Schematic structure of 0.5 ML hydrogen occupying Fe-bridge sites on a magnetic Fe/Ir(001) surface. Squares mark the topmost Ir substrate atoms, circles mark the Fe atoms (full/empty denote up/down spin), and white triangles mark the hydrogen atoms. Upper panel: Hydrogen atoms occupying either next-neighboring (NN-H) Fe-bridge sites (left frame) or less stable neighboring sites (right frame) on a $p(2 \times 1)$ antiferromagnetic Fe/Ir(001) surface. Lower panel: Different magnetic configurations for hydrogen occupying next-neighboring Fe-bridge sites. The energy differences ΔE with respect to the minimum energy solution is given per H atom in the upper and per Fe atom in the lower panel.

$E_{\mathrm{FM}} - E_{\mathrm{AFM}}^{p(2\times1)} = 38$ meV/Fe atom). For a 0.5 ML oxygen coverage diverse geometrical arrangements are possible.

We considered $c(2 \times 2)$O and $p(2 \times 1)$O adlayers and compared minimum total energies (E_{min}) for the FM and three different AFM configurations: $c(2 \times 2)$ AFM, $p(2 \times 1)$ AFM, and $p(1 \times 2)$ AFM magnetic ordering of Fe moments. Oxygen atoms prefer a $p(2 \times 1)$ type overlayer structure ($\Delta E_{\mathrm{tot}} = E_{\mathrm{min}}^{c(2\times2)\mathrm{O}} - E_{\mathrm{min}}^{p(2\times1)\mathrm{O}} = 65$ meV/O atom), the lowest total energy has been found for the $p(1 \times 2)$ AFM magnetic ordering of Fe moments ($E_{\mathrm{AFM}}^{p(2\times1)} > E_{\mathrm{AFM}}^{c(2\times2)} > E_{\mathrm{FM}} > E_{\mathrm{AFM}}^{p(1\times2)}$, $\Delta E_{\mathrm{tot}} = E_{\mathrm{FM}} - E_{\mathrm{AFM}}^{p(1\times2)} = 7$ meV/Fe atom).

In contrast to oxygen, hydrogen atoms prefer Fe-bridge sites on the Fe/Ir(001) surface as shown schematically in Fig. 2.

Similar to oxygen adsorbates, different geometrical arrangements are possible for a 0.5 ML coverage. In our model calculations we considered two H adlayer geometries, H atoms occupying neighboring (N-H) or next-neighboring Fe-bridge (NN-H) sites. Again the energies for FM and three AFM ordered states are compared, i.e., for a $c(2 \times 2)$ AFM, a $p(2 \times 1)$ AFM, and a $p(1 \times 2)$ AFM magnetic ordering of Fe moments. Our calculations show that H atoms prefer to occupy next-neighboring (NN-H) Fe-bridge sites ($\Delta E_{\mathrm{tot}} = E_{\mathrm{min}}^{\mathrm{N\text{-}H}} - E_{\mathrm{min}}^{\mathrm{NN\text{-}H}} = 58$ meV/H atom) and the ground state is obtained for a $p(2 \times 1)$ AFM magnetic ordering of Fe moments (H atoms between parallel Fe moments). Figure 2 shows the magnetic ordering with $E_{\mathrm{AFM}}^{p(1\times2)} > E_{\mathrm{FM}} > E_{\mathrm{AFM}}^{c(2\times2)} > E_{\mathrm{AFM}}^{p(2\times1)}$, and $\Delta E_{\mathrm{tot}} = E_{\mathrm{AFM}}^{c(2\times2)} - E_{\mathrm{AFM}}^{p(2\times1)} = 5$ meV/Fe atom). The optimized geometry further showed that an unsymmetrical (N-H) occupation of bridge sites on the Fe/Ir(001) surface induces considerable buckling in the subsurface Ir layer ($b_3 = 0.17$ Å).

We suppose that under real conditions the hydrogen adsorption starts for lower coverage ($\Theta \approx 0$) with a random occupation of bridge sites. By increasing the H coverage ($\Theta \rightarrow 1$) the ordering of adsorbed H atoms starts to support the $p(2 \times 1)$ magnetic structure. Nevertheless, the formation of domains can be expected rather than a long-range order.

B. Electronic structure

Here we wish to discuss the changes induced by hydrogen and oxygen adsorption on the Fe/Ir(001) surface as reflected in the local density of states (LDOS). We only show results for the structural and magnetic configurations with the lowest energy as determined in the previous subsection. The changes induced by the H and O adsorption is best discussed by comparing with the clean reference Fe/Ir(001) system for which in Refs. 3 and 4 a complex magnetic ground state (chiral magnetic structure) was predicted.

In Fig. 3 we compare the LDOS for a $c(2 \times 2)$ AFM ordered Fe on Ir(001) with the Fe/Ir(001) system in the DLM state, which can be considered as a "disordered" AFM state. In order to exclude the effects of different interlayer distances, the same geometry was used in both cases. We find a good overall agreement between both LDOS (main peaks, the widths), which means that if we find relevant changes between the reference Fe/Ir(001) system and its counterpart with adsorbed O or H atoms, these changes reflect mostly changes induced by adsorbate-Fe hybridization[6] rather than small differences between similar magnetic configurations.

The effect of the oxygen adsorption on Fe/Ir(001) is shown in Fig. 4 for 1 ML O and it is compared with the reference $c(2 \times 2)$ Fe on the Ir(001) surface (no oxygen). In both cases fully relaxed geometries were used. The most important effect shown in Fig. 4 is a strong change of the LDOS features due to the oxygen-iron hybridization. The effect is stronger for majority states as compared to minority states similar to oxygen-covered bcc-Fe(001).[6] In Fig. 5 we show the LDOS for an ordered half-monolayer of oxygen.

While the overall shape of the LDOS is similar for the two oxygen coverages, some changes can be traced down in the vicinity of the Fermi level (see insets in Figs. 4 and 5 showing

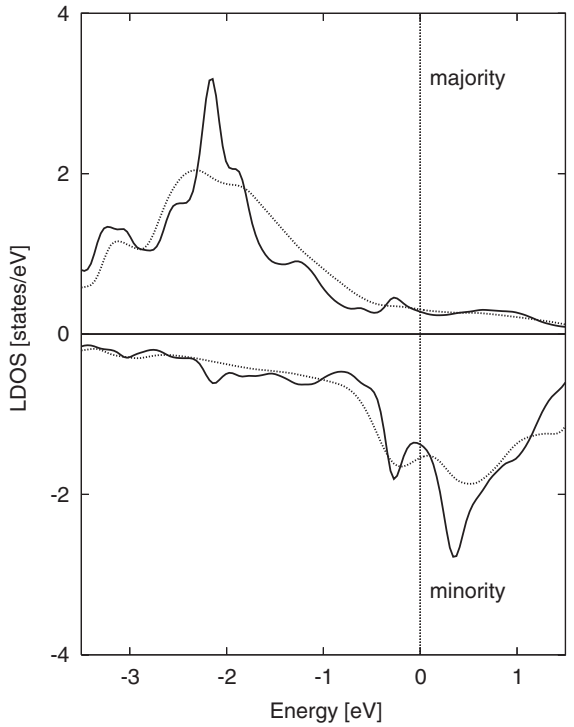

FIG. 3. Spin resolved local density of states (LDOS) of an Fe atom in Fe/Ir(001): (i) $c(2 \times 2)$ AFM (full lines), and (ii) DLM solution (dotted lines) for the experimental geometry and E_F set to zero.

in detail the density for minority states). The changes in the LDOS due to the oxygen-iron wave function hybridization as described above are a precursor of differences in their magnetic stability (see Fig. 8 below).

The effect of hydrogen adsorption on the LDOS is similar to oxygen as shown for the adsorption of 0.5 ML H in Fig. 6.

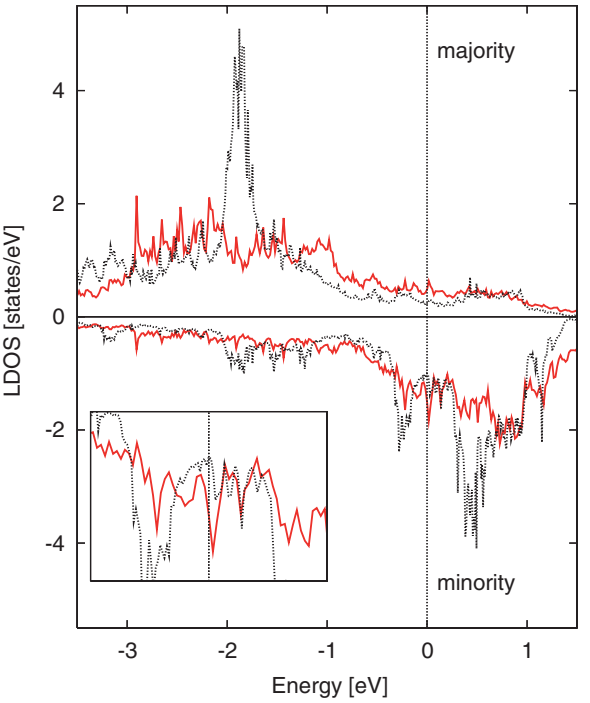

FIG. 5. (Color online) The same as in Fig. 4 but for a $p(1 \times 2)$ ordered half-monolayer oxygen coverage (full lines).

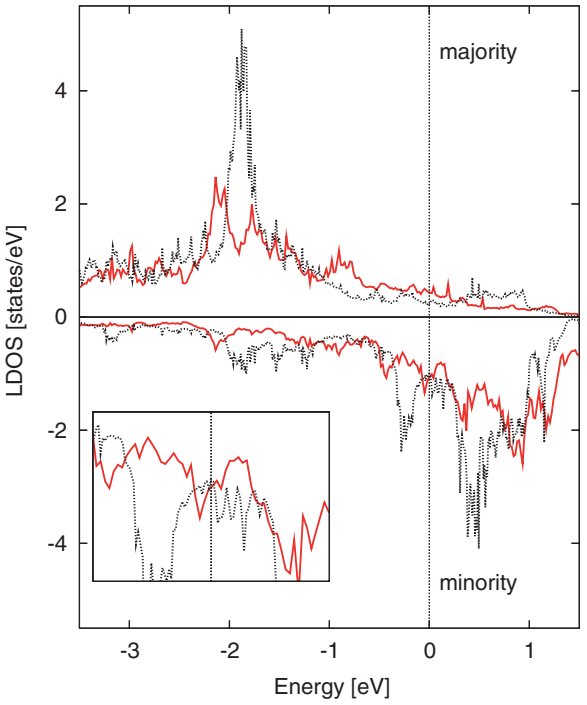

FIG. 4. (Color online) Spin resolved local density of states (LDOS) of an Fe atom of antiferromagnetic $p(2 \times 1)$ Fe/Ir(001) covered by an oxygen monolayer (full lines) compared to the clean antiferromagnetic $c(2 \times 2)$ Fe/Ir(001) system (dotted lines). The inset shows the vicinity of the Fermi level ($E_F = 0$) for minority states.

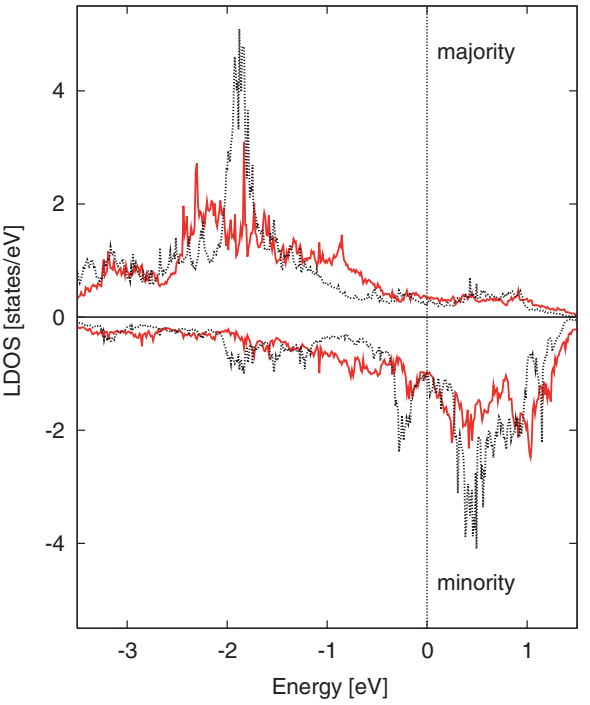

FIG. 6. (Color online) Spin resolved local density of states (LDOS) of an Fe atom of antiferromagnetic $p(2 \times 1)$ Fe/Ir(001) covered by half a monolayer of hydrogen (full line) compared to the clean antiferromagnetic $c(2 \times 2)$ Fe/Ir(001) system (dotted lines) and E_F set to zero.

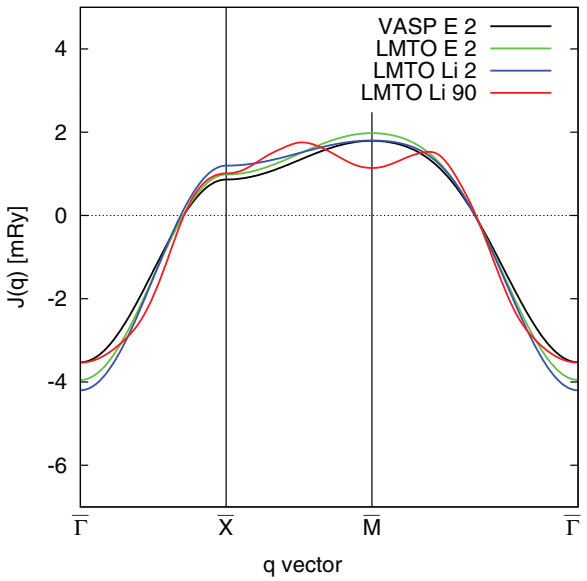

FIG. 7. (Color online) Lattice Fourier transform of the real-space exchange interactions $J_{ij}^{\mathrm{Fe,Fe}}$, $J(\mathbf{q}_\parallel)$, for the clean reference Fe/Ir(001) system in the relaxed minimum energy geometry obtained from total energy and DLM approaches. Total energy approach using VASP (VASP E 2) and TB-LMTO (LMTO E 2). DLM approach using TB-LMTO and just two exchange integrals (LMTO Li 2) or TB-LMTO with 90 exchange integrals (LMTO Li 90).

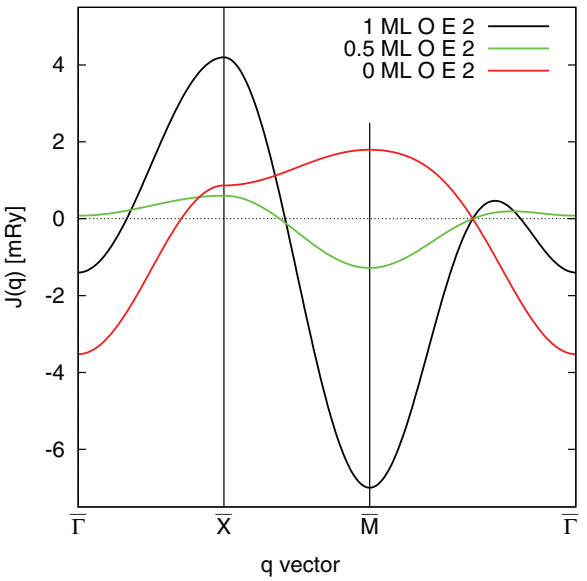

FIG. 8. (Color online) Lattice Fourier transform of real-space exchange interactions $J_{ij}^{\mathrm{Fe,Fe}}$, $J(\mathbf{q}_\parallel)$, for clean antiferromagnetic $c(2\times 2)$ Fe/Ir(001) (0 ML O E 2) and covered by half a monolayer of oxygen (0.5 ML O E 2) and an oxygen monolayer (1 ML O E 2). The oxygen atoms occupy fourfold Fe hollow sites.

We again see mostly a broadening of LDOS peaks due to the Fe-H interaction.

C. Magnetic phase stability

We study the magnetic phase using the lattice Fourier transform of the real-space exchange integrals estimated using the total energy and DLM models, as shown in Fig. 7. We start with the reference case of the Fe/Ir(001) system studied previously in the framework of the DLM model,[3] but compare it here with its total energy model counterparts [see Eq. (1)]. The corresponding total energies have been obtained both from VASP and TB-LMTO calculations. The DLM approach is shown here for two cases with vastly different numbers of exchange integrals included in the lattice Fourier transform, namely for 90 integrals and for just the two leading terms (two shells of neighbors). It should be noted that the DLM exchange integrals correspond to bare ones while those obtained from total energies are effective ones which in some sense combine all of them into two terms.

We see an overall good agreement between both approaches, nevertheless in the full DLM approach (90 shells) the ground state moves from the antiferromagnetic $c(2\times 2)$ state (the $\bar{M}$-ordering vector) to a more complex magnetic state with an ordering vector lying on the $\bar{X}$-$\bar{M}$ line. We also note that both the $p(2\times 1)$ AFM state (the $\bar{X}$-ordering vector) and $c(2\times 2)$ AFM state are energetically close, while the ferromagnetic state (the $\bar{\Gamma}$ -ordering vector) is energetically higher [due to the adopted convention for the Heisenberg Hamiltonian[3] the lowest energy corresponds the maximum of the $J(\mathbf{q}_\parallel)$ curve].

1. O and H adsorption: Total energy model

The lattice Fourier transform for the oxygen adsorption is shown in Fig. 8 and compared with the reference oxygen-free case.

We see that 1 ML oxygen induces a $p(2\times 1)$ antiferromagnetic state (the $\bar{X}$-ordering vector) in contrast to the $c(2\times 2)$ antiferromagnetic state (the $\bar{M}$-ordering vector) originally considered for the clean surface. The high stability of the $p(2\times 1)$ state is strongly reduced for a half-monolayer oxygen coverage. Interestingly the ferromagnetic state is energetically rather close to the ground state, which can be ascribed to the interplay between Fe-O hybridization which promotes a $p(2\times 1)$ state and the increase of the Fe-Ir distance upon O adsorption. The ferromagnetic state is the ground state for large Fe-Ir interlayer distances in the Fe/Ir(001) system.[3]

The energetic ordering can be understood, at least qualitatively, by applying the Kanamori-Goodenough-Anderson[13–15] rules in a simple way. These rules predict that Fe-O-Fe bond angles of 90° favor a ferromagnetic (FM) coupling of the Fe atoms, while Fe-O-Fe bond angles of 180° favor an antiferromagnetic (AFM) one. We apply now these rules for the 1 ML O overlayer as depicted in the top panel of Fig. 1. The preferred magnetic coupling is a result of magnetic interactions between neighboring Fe atoms (Fe-O-Fe bond angles 85°) and next-neighboring Fe atoms (Fe-O-Fe bond angles 146°). For the present purpose, the values of 85° and 146° for the calculated minimum energy geometry are sufficiently close to the ideal values of 90° and 180°. Summing up neighboring and next-neighboring Fe couplings one easily finds that for the most stable AFM $p(2\times 1)$ state one half of the 85° couplings are favorable while the other half are unfavorable, whereas both 146° couplings are favorable. In case of the FM configuration the favorable 85° couplings are offset by unfavorable 146° FM couplings. For AFM $c(2\times 2)$

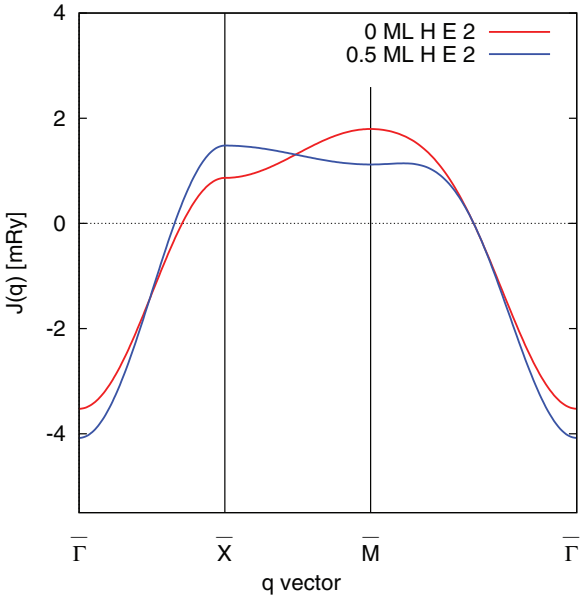

FIG. 9. (Color online) Lattice Fourier transform of real-space exchange interactions $J_{ij}^{\mathrm{Fe,Fe}}$, $J(\mathbf{q}_\parallel)$, for the Fe/Ir(001) system covered by half a monolayer of hydrogen (0.5 ML H E 2). The magnetic ground state is obtained for an antiferromagnetic $p(2 \times 1)$ ordering of Fe the moments. The hydrogen-free clean antiferromagnetic $c(2 \times 2)$ Fe/Ir(001) system (0 ML H E 2) is shown for comparison.

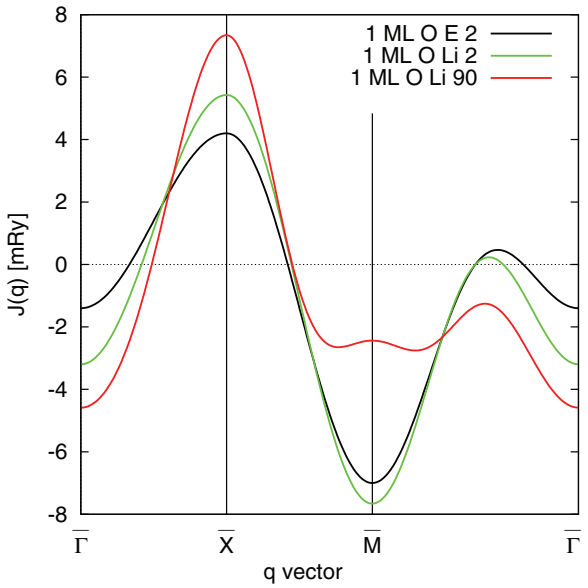

FIG. 10. (Color online) Lattice Fourier transform of the real-space exchange interactions $J_{ij}^{\mathrm{Fe,Fe}}$, $J(\mathbf{q}_\parallel)$ for the Fe/Ir(001) covered by the 1 ML of oxygen determined in the framework of the DLM approach is compared to results from a total energy approach using VASP (1 ML O E 2). Compared are two different TB-LMTO based DLM approaches, one with just two exchange integrals (LMTO Li 2) and the other with all 90 calculated exchange integrals (LMTO Li 90).

all couplings are unfavorable, indicating a predominance of Fe-O-Fe induced couplings over the substrate related $c(2 \times 2)$ AFM coupling of the Fe atoms, which is also offset by the increased Fe/Ir distance upon O adsorption. In summary one can safely state that oxygen adsorption on the Fe/Ir(001) surface strongly influences the magnetic ordering in the Fe monolayer. Turning now to the influence of hydrogen adsorbed at the preferred Fe-bridge sites on the magnetic state, the results for the lattice Fourier transform are summarized in Fig. 9.

A weak preference for the antiferromagnetic $p(2 \times 1)$ state ($\bar{X}$-ordering vector) is seen, as expected from the total energy calculations but the antiferromagnetic $c(2 \times 2)$ state ($\bar{M}$-ordering vector) is energetically quite close. These results suggest that the effect of H adsorption on the magnetic state of Fe/Ir(001) is weaker as compared to the O adsorption. This is also accompanied by a weaker influence on the geometrical structure.

2. O adsorption: DLM model

In this subsection we present results for the magnetic stability of the oxygen monolayer as determined from the DLM model. We wish to point out that the TB-LMTO-DLM model employs the spherical charge approximation which is less accurate as compared to the full potential methods like VASP. We have shown, however, that for layer relaxations up to 15% of the interlayer distance [the case of Fe/Ir(001)[3]] the results obtained using the total energy and TB-LMTO methods are in good agreement (see Fig. 7 and discussion therein). However, the situation for an O monolayer is worse as the O-Fe interatomic distance amounts to only 2.01 Å (as compared to the host interatomic distance of 2.72 Å). The problem in our TB-LMTO model consists of the division of the space into vacuum, oxygen, and iron spheres, which is not unique. We have therefore used the same approach as in our previous work.[3] A similar approach used recently for the oxygen adsorption on bcc-Fe(001) has lead to a qualitative agreement with experiment. In Fig. 10 we present results for 1 ML O on Fe/Ir(001) and compare them with the results of the supercell VASP approach as presented in Fig. 8.

Like in Fig. 7, we tested the dependence of the magnetic stability on the number of shells included in calculations of the lattice Fourier transform. The most important conclusion, namely, that the oxygen monolayer stabilizes the antiferromagnetic $p(2 \times 1)$ ground state for Fe/Ir(001), was unambiguously obtained in both approaches. In addition, even quantitative agreement is satisfactory although the differences for various number of shells included in the DLM method are larger as compared to the oxygen free case (see Fig. 7). On the other hand, there is no indication of a more complex magnetic state if the number of included exchange interactions is increased.

D. Scanning tunneling microscopy

Surprisingly, the simulated constant current STM images shown in Fig. 11 resolve the $p(2 \times 1)$ AFM magnetic ordering of the Fe atoms even for a simulation assuming an unpolarized tip in the Tersoff-Hamann model. Although a spin polarized tip could directly deal with the different orientation of the Fe moments, the AFM ordering of the Fe atoms as imprinted on the O atoms by hybridization may be also detected by a nonmagnetic tip. For small bias voltages, ± 100 meV around E_{F}, the consequences of magnetic Fe-O hybridization are clearly visible in the corrugation of the O atoms. Scanning

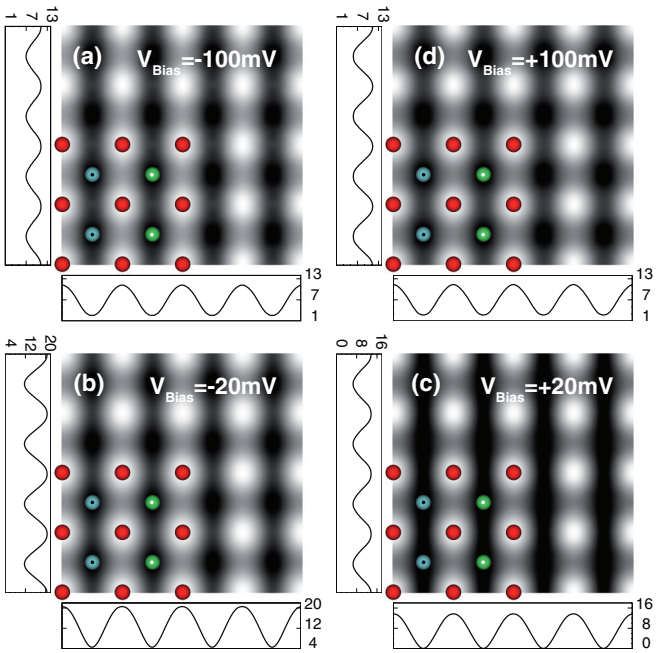

FIG. 11. (Color online) (a)–(d) Simulated (Tersoff-Hamann model) constant current STM images of 1 ML O on an antiferromagnetic $p(2 \times 1)$ Fe/Ir(001) surface for bias voltages V_{Bias} around E_{F}. Red spheres denote the positions of the O atoms, blue and green spheres mark Fe atoms with up and down moments, respectively. Simulated line scans across the oxygen rows are drawn outside each image. A different corrugation for scans either parallel to FM or AFM ordered Fe atom rows is clearly visible, highlighting the $p(2 \times 1)$ AFM ordering. The chosen charge density contour leads to tip-sample distances of ∼3–4 Å (above the O atoms).

above oxygen rows either parallel to FM oriented Fe rows or AFM oriented Fe rows, leads to corrugation differences of up to 8 pm, as shown in the simulated line scans in Fig. 11. Resolving such differences is certainly possible for experimental STM scans and thus should yield direct information on the predicted magnetic ordering.

IV. CONCLUSIONS

We have investigated the effect of oxygen and hydrogen adsorption on the structural and magnetic properties of an Fe/Ir(001) system from first principles. While the structural part was solved using an supercell VASP approach, we used two complementary approaches for the prediction of the magnetic state: A total energy model using supercell VASP calculations and the TB-LMTO-DLM method working with the semi-infinite geometries. The emphasis was put on the influence of the O and H adsorption on the magnetic stability. The following main conclusions can be drawn: (i) Oxygen adsorbs on the Fe/Ir(001) surface at fourfold hollow Fe sites and influences the atomic geometry (interlayer distances) of the system more strongly than hydrogen adsorbing at Fe-bridge positions. In particular, the adsorption of an oxygen monolayer strongly increases the interlayer distance between Fe and the top Ir layer. (ii) The oxygen-iron hybridization mainly broadens density of states features as compared to the clean surface. This change of the electronic structure manifests itself in corresponding modifications of exchange interactions and the STM current. (iii) The magnetic stability is influenced by oxygen adsorption, and we predict an antiferromagnetic $p(2 \times 1)$ magnetic ground state with a $\bar{X}$-ordering vector as obtained by two complementary approaches, namely supercell VASP and DLM model. (iv) The $\bar{X}$ ordering is weakened by decreasing oxygen coverage and changes into a complex magnetic ground state for oxygen-free Fe/Ir(001). (v) Hydrogen adsorption leads to a weak stabilization of an antiferromagnetic $p(2 \times 1)$ order. (vi) STM images for nonmagnetic tips reflect the $p(2 \times 1)$ AFM ordering of the Fe moments not directly, but rather by hybridization with the O atoms, best visible for small bias voltages.

ACKNOWLEDGMENTS

F.M., J.K., and V.D. acknowledge support of the Czech Science Foundation (Projects IAA100100912 and P202/09/0775). J.R. is grateful for financial support from the Austrian Science Fund (FWF) SFB ViCoM F4109-N13 and for computer support of the Vienna Scientific Cluster (VSC).

*maca@fzu.cz

[1] V. Martin, W. Meyer, C. Giovanardi, L. Hammer, K. Heinz, Z. Tian, D. Sander, and J. Kirschner, Phys. Rev. B **76**, 205418 (2007).
[2] V. Martin, Diplomarbeit, Institut für Physik der Kondensierten Materie der Friedrich-Alexander-Universität Erlangen-Nürenberg, 2006.
[3] J. Kudrnovský, F. Máca, I. Turek, and J. Redinger, Phys. Rev. B **80**, 064405 (2009).
[4] A. Deák, L. Szunyogh, and B. Ujfalussy, Phys. Rev. B **84**, 224413 (2011).
[5] P. Ferriani, K. von Bergmann, E. Y. Vedmedenko, S. Heinze, M. Bode, M. Heide, G. Bihlmayer, S. Blügel, and R. Wiesendanger, Phys. Rev. Lett. **101**, 027201 (2008).
[6] A. Tange, C. L. Gao, B. Yu. Yavorsky, I. V. Maznichenko, C. Etz, A. Ernst, W. Hergert, I. Mertig, W. Wulfhekel, and J. Kirschner, Phys. Rev. B **81**, 195410 (2010).
[7] G. Kresse and J. Furthmüller, Phys. Rev. B **54**, 11169 (1996).
[8] M. Mašín, L. Bergqvist, J. Kudrnovský, M. Kotrla, and V. Drchal, Phys. Rev. B **87**, 075452 (2013).
[9] J. Tersoff and D. R. Hamann, Phys. Rev. B **31**, 805 (1985).
[10] G. Kresse and D. Joubert, Phys. Rev. B **59**, 1758 (1999).
[11] J. P. Perdew and A. Zunger, Phys. Rev. B **23**, 5048 (1981); D. M. Ceperley and B. J. Alder, Phys. Rev. Lett. **45**, 566 (1980).
[12] I. Turek, J. Kudrnovský, V. Drchal, and P. Bruno, Philos. Mag. **86**, 1713 (2006).
[13] J. Kanamori, J. Phys. Chem. Solids **87**, 10 (1959).
[14] J. B. Goodenough, Phys. Rev. **117**, 1442 (1960); *Magnetism and the Chemical Bond* (Interscience, New York, 1963).
[15] P. W. Anderson, Solid State Phys. **14**, 99 (1963).